Physical, water diffusion and micro-structural analysis of "Canarium schweinsfurthii Engl"

Bernard Morino Ganou Koungang[1,2,*], Dieunedort Ndapeu[1,*], Gilbert Tchemou[1], Paul William Huisken Mejouyo[1], Bernard Wenga Ntcheping[1], Josepha Tendo Foba[1], Luc Courard[2], Ebenezer Njeugna[1]

[1]Laboratoire de Mécanique et Matériaux Adaptés (LAMMA), Université de Douala, 1872 Douala-Cameroun
[2]Urban and Environmental Engineering (UEE), Laboratoire des Matériaux de Construction (LMC), Université de Liège (ULiège), Allée de la Découverte, 9, 4000 Liège, Belgique
*Corresponding author : ndapeu@gmail.com; morinoganou@yahoo.fr

How to cite this paper: B.M. Ganou Koungang, D. Ndapeu, G. Tchemou, P.W. Huisken Mejouyo, B. Wenga Ntcheping, J.T. Foba, L. Courard, E. Njeugna (2020) Physical, water diffusion and micro-structural analysis of "Canarium schweinfurthii Engl". ******, *****, *-*.
https://dx.doi.org/10.4236/***.2020.*****

Received: **** **, ***
Accepted: **** **, ***
Published: **** **, ***

Abstract

The purpose of this study is to determine the morphological, microstructural characteristics and water diffusion parameters of the Canarium schweinfurthii (CS) shellnut. This work is part of a vast project to valorize the above-mentioned cores for possible industrial use as charges in composites or abrasives materials. The study was based on the characterization of intrinsic physical characteristics of the coreshells scanning electron microscopic (SEM) observations desorption, adsorption and absorption kinetics. The water diffusion phenomenon was modeled and it appears that the Page model well predicted the kinetic of drying, absorption and adsorption. The effective diffusion coefficient and the energy of activation were calculated at three isothermal temperatures (50, 70 and 90°C). There was a tendency for hysteresis in the sorption-desorption cycles. These results strongly predicted the possibility of using these products as a filler in composites, clay building materials and cement because of their high water diffusion stability on a macroscopic scale.

Keywords

Bioresources, shellnut, Canarium schweinfurthii Engl, microscopy, water absorption, moisture adsorption, desorption

1. Introduction

The need to develop new construction materials is a major challenge for scientists in this century. The Canarium schweinfurthii Engl (CS) is a large tree (Fig. 1a) widespread in sub-Saharan Africa [1], [2]. It has a height that can reach 25 to 40 m and a trunk about 1.50 m in diameter. It is covered with a clear bark about 1 cm thickness, which allows it to exude a fragrant resin that becomes opaque in air [3].

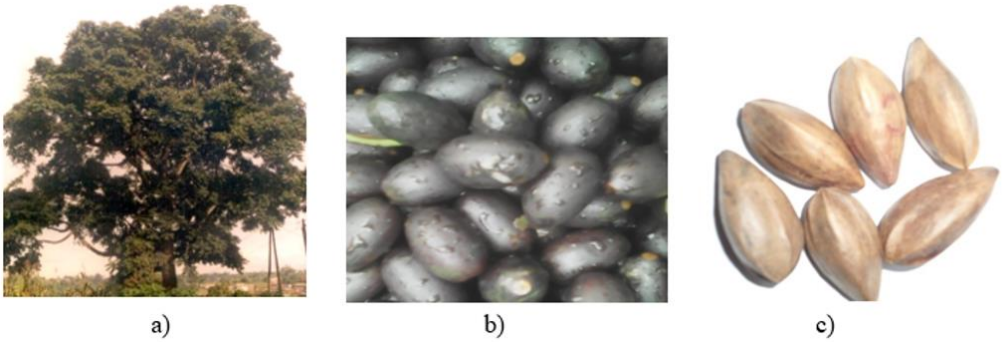

Figure 1. CS: a) tree, b) fruits, c) cores.

The CS tree is an oilseed producer belonging to the Burseraceae family and it is of great importance in the African culture. Indeed, it is a potential source of lipids with an outer seed pulp of about 40% fat [4]. In the socio-cultural and economic domain its fruits (Fig. 1b) commonly called "black fruits" in Cameroon, are traded in the market of the West region of Cameroon. Its by-products and derivatives are used in the pharmacopeia area. In the recent research, there is not statistical data quantify the waste of this product. In the daily life in Africa, this fruit is consumed by the populations. Waste is observed in markets and public landfills. However, several research studies have leaned towards promoting it in the food, pharmacopoeia and recycling fields [5]. The literature review on CS fruits showed that they have many virtues and uses [4]: it is a source of food, medicine, income, and cultural wealth. The pulp is consumed after softening as fruit. It can also be used in pastries. The high oil content of the fruits makes it a potential source of lipids[6]. Its high production period, which extends over 7 months from September to March [7], is very long. The production of CS Engl. pulp fruit is about one thousand tons by year for the national harvest [8].

Most papers have reported the development of activated charcoals based on CS kernels (Fig. 1c) [9]–[11] for use as an absorbent in filters for copper II ions and other heavy ions. Recent work is indeed interested in using CS aggregates as a filler for composite materials [12].

In the field of physical characterization, Noumi et al. (2004) have studied kinetic of global Canarium schweinfurthii Engl. pulp fruit, under conditions of air velocity ranging between 1m/s and 3 m/s, relative humidity between 40% and 60%, temperature between 40°C and 70 °C [13]. Similarly, Chinaka Ehiem et al. (2019) focused their study in the predicting of suitable water absorption of global C.S pulp fruit at three different temperatures (35°C, 50°C, 65°C) [14]. Very few or no researchers have so far focused on the CS core (part 1 fig.2) which could be a material with interesting properties for the particle composite industry [12]. It is therefore interesting to study the intrinsic properties of this by-product in order to consider its use.

The literature allowed us to clearly orient our objective in particular the choice to make research on a specific part of the fruit (Part1 Fig.2) whose recycling could be useful for several sectors like abrasion, braking, and in wherever possible insertion in powder form

as aggregates of composite materials.

The purpose of this work is to study the morphology and microstructure of the CS core and to analyze its capacity for water and moisture uptake and desorption, based on empirical models widely found in the literature. This study will make it possible to predict the behavior of CS both in the development of liquid-bonded composites and in the face of environmental hydric conditions.

2. Materials and methods

2.1. Materials: CS shellnut

The CS fruit is a small blue-violet drupe, being about 3–4 cm in length and 1–2 cm in thickness (Fig. 2a). The calyx shell is persistent and remains attached to the fruit. The fruit contains a hard core, shaped like a trillium spindle, with one seed. The fleshy and edible pulp covers a nucleus 2.5 cm long and 1 to 1.5 cm in diameter. After the consumption of the pulp, the shellnuts are commonly abandoned in the environment (Fig. 2b).

In order to obtain useful test specimens for characterizations, the first step is a special operations of core treatments. (Fig. 3). The steps listed in Fig. 3 show the main operations for obtaining usable aggregates by treating the shellnut devoid of the pulp (Fig. 2b) and other dirt (Fig. 2c, 2d), starting from the basic fruit (Fig. 1b) to the crushed aggregates (Fig. 2e).

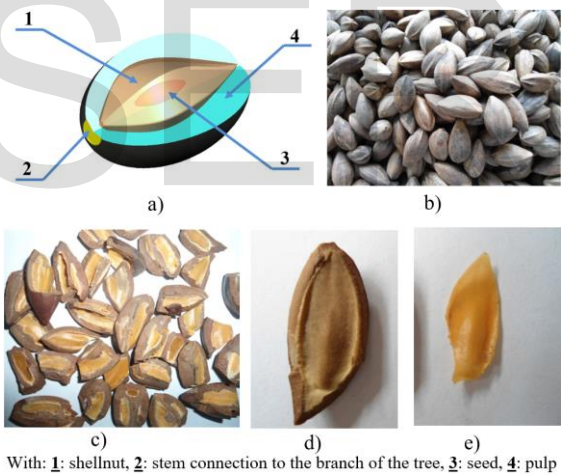

Figure 2. CS fruit: a) sectional view of the fruit [12], b) cleaned cores Crushed kernels: c) with inner layer, d) without inner layer, e) inner layer.

2.2. Obtaining test specimens

2.2.1. Process description

Obtaining specimens to be used for the physical characterization required four main steps to ensure and warrant a reproducible result: external and internal cleaning of the coreshell, sawing by clamping with a vice and, finally, shaping to smoothen all the core surfaces by sand paper.

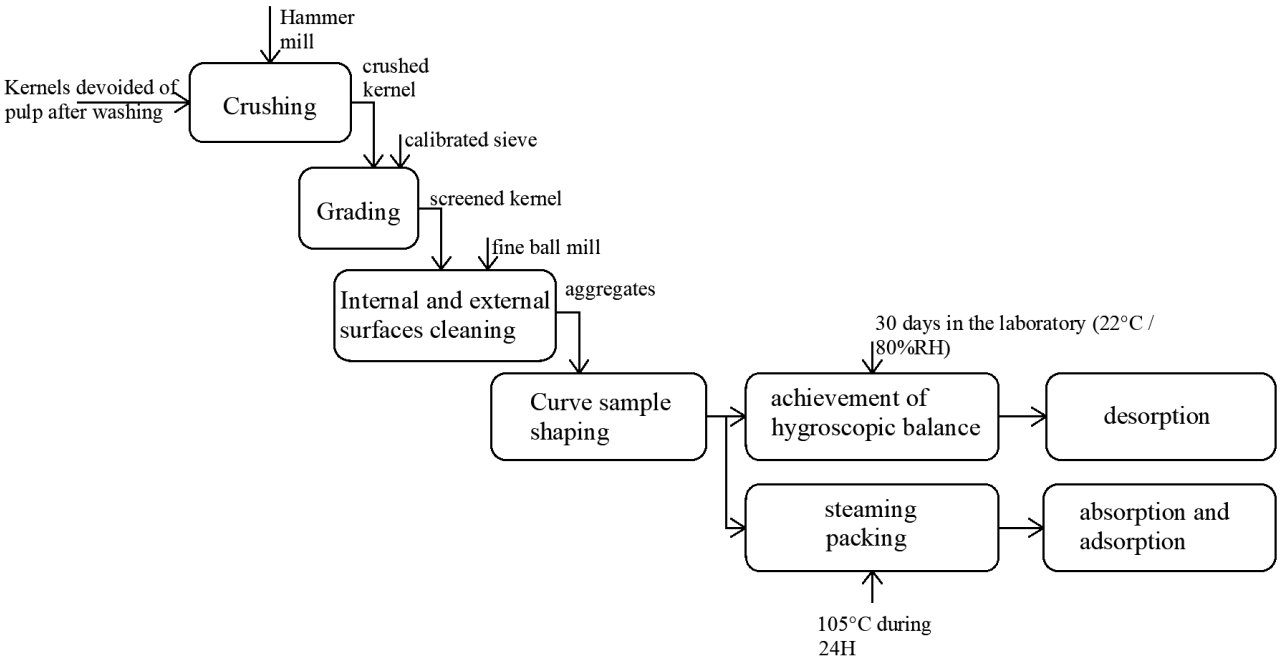

Figure 3. Process flowchart.

Curved samples (14 for each experimentation) of the cores shells were prepared (Fig. 4a) for sorption and desorption analysis. This particular curved geometry of the samples is imposed by the form of the CS-shellnut. This shape also permits the use of the Crank solution of the partial equation for water diffusion through the material.

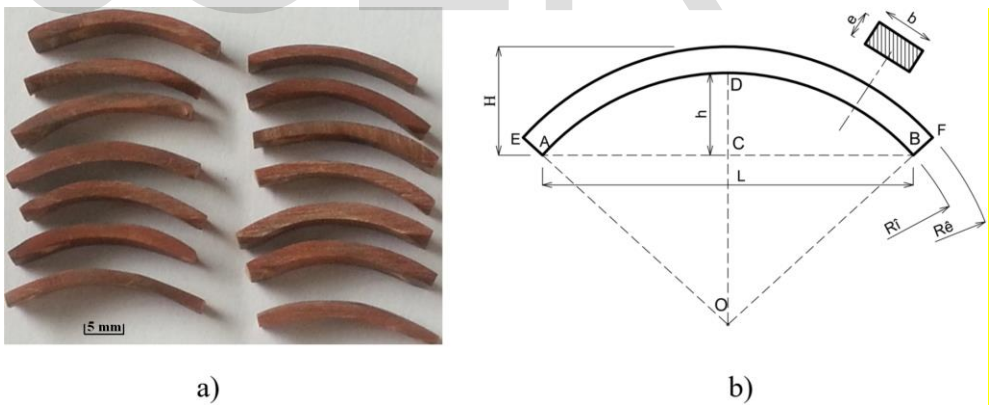

Figure 4. Test specimens for sorption and desorption tests: a) samples, b) pattern parameters of the curved specimens.

2.2.2. Determination of the shape parameters R_i and R_e

The samples were cut into curved shaped section, as shown in Fig.4a. For each specimen, the inner R_i and outside R_e radii were determined according to the shape parameters shown in Fig. 4b. The inner bending radius was obtained on the basis of the pythagorean theorem for the right triangle OCA. The following equations were used:

$$OA^2 = OC^2 + CA^2 \quad (1)$$

$$R_i = \frac{1}{2}\left(h + \frac{L^2}{4h}\right) \quad (2)$$

$$R_i = \frac{1}{2}\left(h + \frac{L^2}{4h}\right) + e \quad (3)$$

With: L: Chord to the inner circle, e: Thickness of the section, H: Height of the straight section taken in line of external curvature, h: Height of the straight section taken in line of internal curvature, R_e: Outside radius of curvature, R_i: Inner radius.
The values of $R_e \approx 26$ mm and $R_i \approx 24$ mm were obtained.

2.3. Microscopic characterization

The observation of CS-shellnut microstructure was performed by using a scanning electron microscope (SEM) model Hitachi SU-8230 Field Emission-STEM (FE-STEM). The CS-shellnut was cut as shown in Fig. 5 along the meridional (MP) and equatorial (EP) planes.

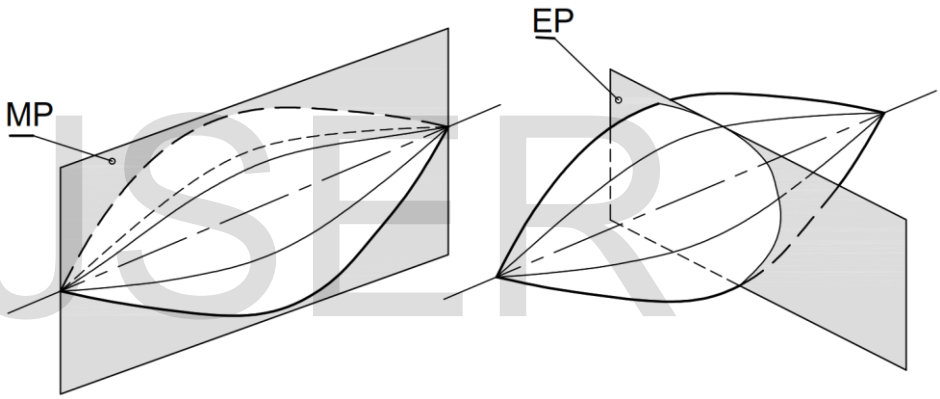

Figure 5. CS-shell cutting planes for SEM observation: a) meridional plane (MP), b) equatorial plane (EP).

2.4. Physical characterization

Initially, it will be a question of determining the true density of 2 mm CS particles at a helium pycnometer. Then the sorption and desorption analyses will be carried out on the curved specimens (Fig.4).

2.4.1. Desorption at 50 °C, 70 °C and 90°C

The 14 specimens with the rectangular torus section shape (Fig. 4a) were initially weighed using a digital scale (PGW Adam 753i with an accuracy of 1:1000e). Isotherms of 50°C, 70°C and 90°C were used for the experiments. These temperatures were chosen below the boiling temperature of water in order to have controlled kinetics [15]. The ventilated oven (Memmert UF110) was turned on and set to idle until stabilized before the specimens were introduced. The samples were kept in the laboratory for 30 days at room temperature about 25°C and 80%HR, to achieve a hygroscopic balance with the environment. They were

weighed to determine their wet mass m_0 due the laboratory exposure before baking. After each 5 minutes of time (t) in the oven, the value m(t) of the sample mass, was recorded. This operation was repeated until stabilization of the recorded mass, m_{eq} [16].
The sorption ratio, noted MR, was determined using equation (4).

$$MR = \frac{m(t) - m_0}{m_{eq} - m_0} \quad (4)$$

Matlab's software was used to analyse the experimental values of desorption at 50 °C, 70°C and 90 °C and correlation with model presented in Table 1.

Table 1. Mathematical models used in drying kinetics

Authors	Models
Newton and Lawis	MR = exp(-kt)
Page	MR = exp(-kt^n)
Henderson and Pabis	MR = aexp(-kt)
Logarithmic	MR = aexp(-kt) + bt
Midilli	MR = aexp(-kt^n) + bt
Verma at al.	MR = aexp(-kt) + (1-a)exp (-gt)
Modified Henderson and Pabis	MR = aexp(-kt) + bexp(-gt) + cexp(-ht)
Peleg	MR = 1- [t / (a + bt)]
Aghbashlo	MR = exp [-kt / (1 + at)]

With: MR: moisture ratio; a, b, g, k, h, n: parameters of the models; t: duration.

2.4.2. Moisture adsorption

The method used for determination of the moisture adsorption was the gravimetric method with discontinuous weighing. Lahsasni et al. (2004) specified that, after conditioning, the 14 specimen are weighed to determine the initial mass and, subsequently, stored on a grill mesh inside an experimental tray (Fig. 6) containing a saturated sodium chloride (NaCl) solution where a relative humidity of 75% and a temperature of 30°C are provided [17].
Matlab's software was used to analyse the experimental values of moisture adsorption at relative humidity of 75% and a temperature of 30 °C. The correlation was done with models presented in Table 2.

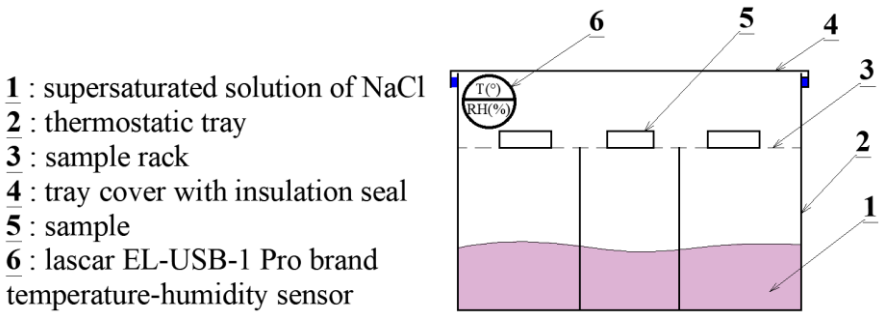

Figure 6. Experimental setup for adsorption tests.

2.4.3. Water absorption

The 14 specimens were conditioned at 105°C for 24 hours [18], duration of obtaining a constant anhydrous mass after consecutive weighing every 4H of time in an oven. They were then weighed to determine their initial dried mass, m_o, and then were immersed in distilled water.

A discontinuous gravimetric method was used. At specific (t) interval time, the specimens were removed from the water, squeezed on an absorbent paper and weighed to have, at each (t) times, the wet mass m(t). The end of the experiment was noted when an equilibrium weight, m_{eq}, of the m(t) values was obtained [19]–[21].

The percentage of water absorption (WA) was also evaluated by the following relation (Eq.5).

$$WA = \frac{m_{eq} - m_0}{m_0} * 100 \quad (5)$$

Matlab's software was used to analyse the experimental values of water absorption and correlation presented in Table 2.

Table 2. Mathematical models used in drying kinetics

Authors	Models
Page	MR = 1-aexp (-kt^n)
Pilosof	MR = a + (bt)/(c + t)
Mohsenin	MR = a (1-exp (- kt)) + (b + ct)
Sikame et al.	MR = c-aexp (- kt) - b exp (- gt)
Peleg	MR = c + t/(a + bt)

With: MR: moisture ratio; a, b, g, k, n: parameters of the models; t: duration.

2.4.4. Activation energy of water desorption

The activation energy is a characteristic factor for diffusion phenomenon. it is obtained from the Arrhenius equation [22] which describes the dependence of the effective diffusion coefficient on the absolute temperature. Fick's equation (Eq. 8) obtained from Crank's equation of diffusion (Eq. 6) [23], which governs the mass diffusion through the material, was used. Assuming that the effective diffusion coefficient does not depend on either the center of gravity or the position of samples.

$$\frac{\partial u(r,t)}{\partial t} = \nabla\left[D(u(r,t),r)\nabla(u(r,t)\right] \quad (6)$$

where u(r, t) is the density of the diffusing material at location r=(x, y, z) and time t. D(u(r,t),r) is the collective diffusion coefficient for density u at location r.

If the diffusion coefficient doesn't depend on the density, i.e., D is constant, then Eq.(6) reduces to the following linear equation:

$$\frac{\partial u(r,t)}{\partial t} = D\vec{\nabla}^2 u(r,t) \quad (7)$$

By correspondence from Eq.7, it is obtained:

$$\frac{\partial MR}{\partial t} = D_{eff}\,\vec{\nabla}^2 MR \quad (8)$$

Where D_{eff} is the effective diffusion coefficient in m2/s and MR is the absorption ratio. The analytical solution of Eq. 8 for radial diffusion in a hollow cylinder ($R_i \leqslant r \leqslant R_e$), was applied in the case where the internal surfaces at $r = R_i$ and external surfaces r = Re are maintained at constant concentrations C_i and C_e, respectively, in such a way that $C_i \neq C_e$. It is assumed that the effective diffusion coefficient is a constant [23]. Under the conditions mentioned above the theoretical solution of the equation of diffusion is given by Eq.9 for desorption and Eq.10 for absorption.

For kinetic desorption:

$$MR = \frac{6}{\pi^2\left(R_i^{\,2} + R_i R_e + R_e^{\,2}\right)}\sum_{n=1}^{\infty}\left\{\left(\frac{R_e\cos(n\pi) - Ri}{n}\right)^2 \exp\left(\frac{D_{eff}\,n^2\pi^2 t}{\left(R_e - R_i\right)^2}\right)\right\} \quad (9)$$

For kinetic absorption:

$$MR = 1 - \frac{6}{\pi^2\left(R_i^{\,2} + R_i R_e + R_e^{\,2}\right)}\sum_{n=1}^{\infty}\left\{\left(\frac{R_e\cos(n\pi) - R_i}{n}\right)^2 \exp\left(\frac{D_{eff}\,n^2\pi^2 t}{\left(R_e - R_i\right)^2}\right)\right\} \quad (10)$$

With: D_{eff} : effective diffusion coefficient (m^2/s); n : positive integer.

The calculation of the effective diffusion coefficient was performed by means of the Arrhenius equation (11).

$$D_{eff} = D_0 \exp\left(-\frac{E_a}{RT}\right) \quad (11)$$

$$Ln\left(D_{eff}\right) = Ln\left(D_0\right) - \left(\frac{E_a}{R}\right)\frac{1}{T} \quad (12)$$

With: D_o: pre-exponential factor of the Arrhenius equation (m^2/s); E_a: activation energy; T: temperature, R: ideal gas constant (kJ/mol.K).

By limiting the calculation to the first term of each series (Eq.9 and Eq.10), it is obtained the Eq.13 and Eq.14 given by:

For drying kinetics

$$MR = \frac{6}{\pi^2\left(R_i^{\,2} + R_i R_e + R_e^{\,2}\right)}\left(R_e - R_i\right)^2 \exp\left(\frac{D_{eff}\,\pi^2 t}{\left(R_e - R_i\right)^2}\right) \quad (13)$$

For absorption kinetics

$$MR = 1 - \frac{6}{\pi^2\left(R_i^{\,2} + R_i R_e + R_e^{\,2}\right)}\left(R_e - R_i\right)^2 \exp\left(\frac{D_{eff}\,\pi^2 t}{\left(R_e - R_i\right)^2}\right) \quad (14)$$

For absorption, Eq. 14 can be transform to the Eq.15.

$$MR = \frac{\pi^2\left(R_i^2 + R_i R_e + R_e^2\right) - 6\left(R_e - R_i\right)^2}{\pi^2\left(R_i^2 + R_i R_e + R_e^2\right)} \exp\left(\frac{-D_{eff}\,\pi^2 t}{\left(R_e - R_i\right)^2}\right) \quad (15)$$

The natural logarithm of Eq.13 and Eq.15 permit to obtain a linear relationship between lnMR and the time (t) for the drying kinetic (Eq.16) and for the absorption kinetic (Eq.17).

$$\ln(MR) = \ln\left(\frac{6\left(R_e - R_i\right)^2}{\pi^2\left(R_i^2 + R_i R_e + R_e^2\right)}\right) + \left(\frac{-D_{eff}\,\pi^2}{\left(R_e - R_i\right)^2}\right) t \quad (16)$$

$$\ln(MR) = \ln\left(\frac{\pi^2\left(R_i^2 + R_i R_e + R_e^2\right) - 6\left(R_e - R_i\right)^2}{\pi^2\left(R_i^2 + R_i R_e + R_e^2\right)}\right) + \left(\frac{-D_{eff}\,\pi^2}{\left(R_e - R_i\right)^2}\right) t \quad (17)$$

The slope of linear regression (Eq.16 and Eq.17) makes it possible to calculate D_{eff} according to (Eq.18).

$$\left(slope\right)_{16,17} = \frac{\pi^2 D_{eff}}{\left(R_e - R_i\right)^2} \quad \text{then} \quad D_{eff} = -\frac{\left(R_e - R_i\right)^2}{\pi^2} * \left(slope\right)_{16,17} \quad (18)$$

By using the $(Slope)_{12}$ drawn with three isotherms (50, 70, 90°C) in Eq.12, knowing D_{eff} (Eq.18), the value of the activation energy was calculating with:

$$E_a = R * \left(slope\right)_{16,17} \quad (19)$$

3. Results

3.1. Morphology

A morphological analysis of the CS shellnut shows that its volume was delimited by ellipsoidal surfaces (Fig. 7a, 7b) extending from one end (A) to the other (B) with more or less regular sections (Fig. 7c).

Figure 7. CS physical aspects : a) sketch of exterior surfaces, b) photo, c) cross section.

The samples were characterized by P_i external planes with i varying from 1 to 6 (Fig.7c).

3.2. Microscopic structure

The microstructure analysis was performed with SEM where microscopic images made it

possible to explore both longitudinal and equatorial sections of the CS shellnut. This micrographic analysis was directed towards two 90° opposite sections.

Firstly, the meridional section following MP. (Fig.5a), which gave the images presented in Fig.8a.

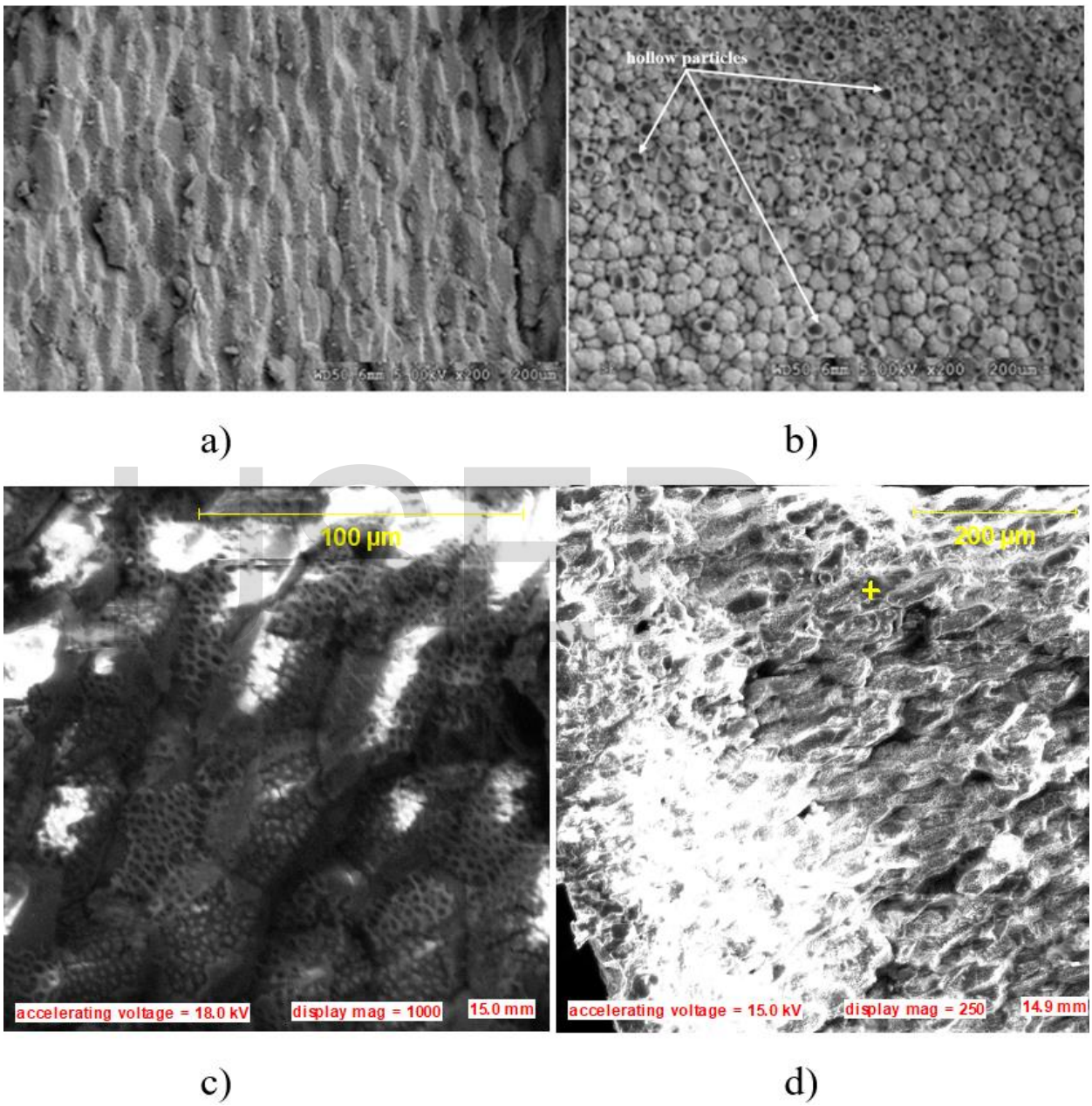

Figure 8. Microstructure: a) longitudinal plane, b) equatorial plane, c) longitudinal plane with high magnitude

Without taking into account the proportion of carbon, EDS analysis (Fig.9, Tab.3) is showing that there is a predominance of light elements of alkaline (Na, K), alkaline earth (Ca)

and halogen (Br) types. The presence in small proportion of a metalloid (Si) induces the non-pouzzolanic character of the ashes which would result from the calcination of the CS nuclei. This composition is typical for low density materials, here the value is 1.30 g/cm^3 which is very close to the density of Cocos nucifera [24].

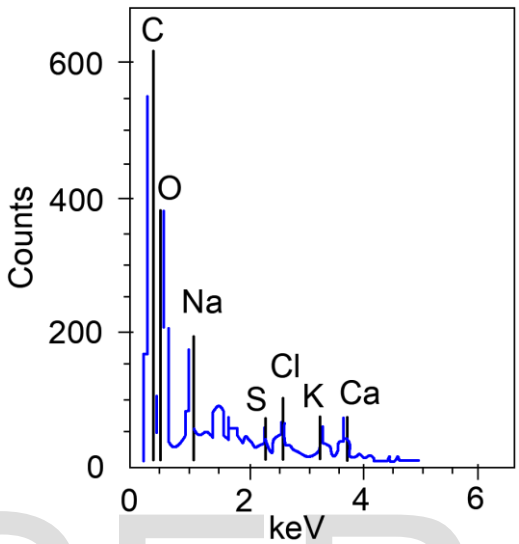

Figure 9. EDS spectrum

Table 3. Mathematical models used in drying kinetics

Other Elements	Na	K	Al	Sn	Si	S	Cl	Br	Ca	Mn	Sr	Ba	Sb	La	Ce
Normalized K-Ratio	29.8	8.7	2.3	5.7	5.0	6.7	6.9	10.4	11.0	1.0	4.4	1.1	4.6	2.0	0.3

An equatorial sections image (Fig.5b) shows relatively close packed shell-shaped hollow particles intermingled with each other like building blocks. The dimension of each particles was of the order of 10µm.

Secondly, the equatorial sections (Fig.8b) confirmed both the recesses observed in the particles during the scanning and the determination of their shell shape. These observations were fundamental in so as they allowed approximations to be made to the granular shape of the particles which make this material a natural and, probably very hard, abrasive, strangely resembling a "pumice" material.

3.3. Drying kinetics

Desorption was carried out at 50°C and 70°C (Fig. 10). The experimental results were compared with various mathematical models (Table 1) using Matlab's software.

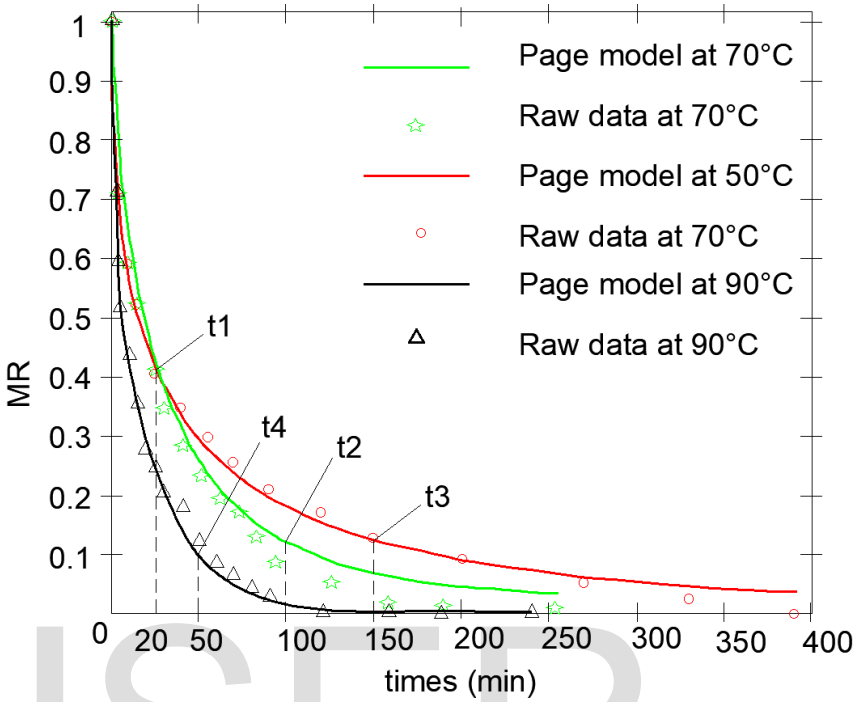

Figure 10. Predicted models of Page for desorption (50°C, 70°C and 90°C).

The model with the best correlation and the lowest error can be selected from Table 4. It presents the average correlation coefficients of the different mathematical models.

Table 4. Comparison of applicability of models in desorption kinetics at 50°C, 70°C and 90°C

Temperature		50° C	70° C	90° C
Statistical indicator		R^2		
Model	Number of parameters			
Newton and Lawis	1.0	0.830	0.953	0.890
Page	2.0	0.994	0.994	0.995
Henderson and Pabis	2.0	0.902	0.974	0.900
Logarithmic	3.0	0.911	0.974	0.888
Midilli	4.0	0.995	0.996	0.962
Verma et al	3.0	0.999	0.997	0.991
Modified Henderson and Pabis	6.0	0.974	0.997	0.918
Peleg	2.0	0.975	0.990	0.953
Aghbashlo	2.0	0.964	0.980	0.959

The Page, Verma et al and Midilli models resulted are showing the best correlation for the three temperatures. On the other hand, by considering the number of parameters of each of the last three models, the one of Page has the fewest parameters and is the simplest. That's

why the Page model was selected for predicting the water desorption from CS shellnut: $MR=\exp(-kt^n)$ with the parameters shown in Table 5.

Table 5. Calculated parameters of Page model for the desorption kinetics

Settings	k	n
Desorption at 50° C	0.178	0.5
Desorption at 70° C	0.096	0.7
Desorption at 90° C	0.245	0.6

With: k, n: parameters of Page model

3.4. Evaluation of effective diffusion coefficient and activation energy

The effective diffusion coefficients were calculated from Eq.17. The average values obtained were $2.70x10^{-11}$ ($\pm$ $2.18x10^{-12}$), $29.71x10^{-11}$ ($\pm$ $1.09x10^{-11}$) $m^2.s^{-1}$ and $39.00x10^{-11}$ ($\pm 2.51x10^{-11}$) $m^2.s^{-1}$, for water desorption at 50°C, 70°C and 90°C, respectively. It is noted that by increasing the temperature by 20°C (between 50°C and 70°C), the diffusion rate was multiplied by a factor of 10, allowing a gain of 50 min of experimentation between 50°C and 70°C and 100 min between 70°C and 90°C.

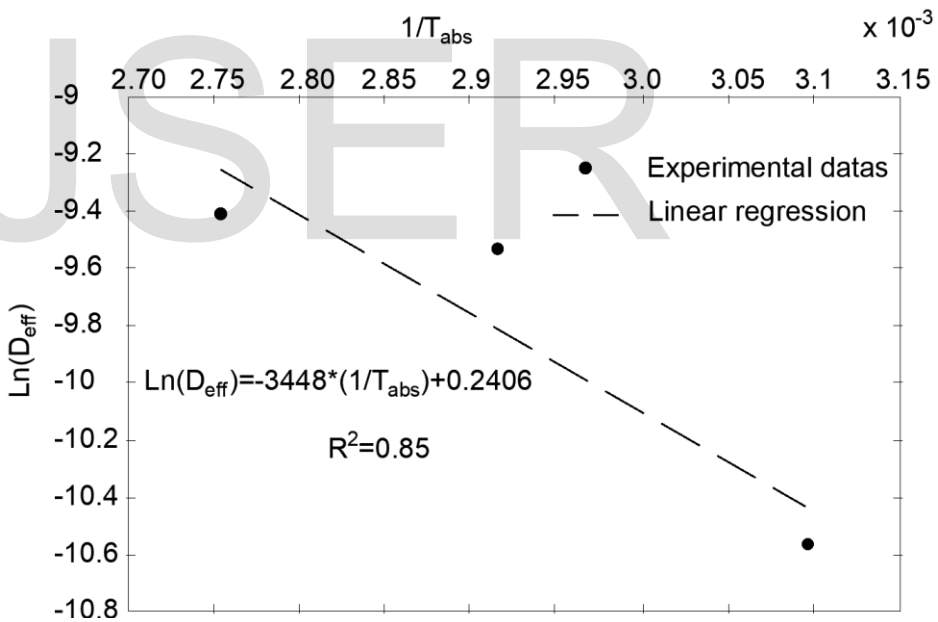

Figure 11. Relation between Deff and 1/Tabs.

The activation energy was calculated from Eq. 19 utilizing the isotherms of 50°C, 70°C and 90°C, it results from the dependence of the coefficient of effective diffusion to the absolute temperature. By using the slope of the line Ln(Deff) in function of 1/Tabs (Fig.11), the value of the activation energy was 28.66 KJ/mol.K. The intercept at the origin of this line permits to deduce the pre-exponential factor D_0 of the Arrhenius equation which was 1.27. Table (5) presents the results of the drying kinetics comparing with Cocos nucifera, almond mature coconut and the fibers of Raphia's leaves [25].

Table 6. Analysis of the drying performance of CS shellnut.

Materials	Cocos nucifera (CN) (Specie 1)	Cocos nucifera (CN) (Specie 2)	Almond mature coconut	Fiber of Raphia's leaves	**CS**
Temperature (°C)	70-180		50-70	30-70	**50-90**
Drying kinetic's model	Midilli		Modified Henderson and Pabis	Page	**Page**
D_{eff} ($m^2.s^{-1}$) (min–max)	$1.46x10^{-8}$–$16.10x10^{-8}$	$1.34x10^{-8}$ – $24.50x10^{-8}$	$0.17x10^{-9}$ –$0.55x10^{-9}$	$3.34x10^{-14}$ – $23.2x10^{-14}$	**$2.70x10^{-11}$ - $39.00x10^{-11}$**
E_a (KJ/mol.K)	31.69	34.46	25.94	49-71	**28.66**
Reference	[16]		[26]	[25]	**Studied case**

The results of the effective diffusion coefficients and activation energy of CS are less than the one of CN which are also a hard shellnut. This observation could be justified on the basis of the porosity distribution, the dense microstructure and the proportion of cellulose or hemicellulose in the shell which is the main factor influencing this parameter [27]–[29].

The adopted model of Page was used to plot and compare the desorption curves at 50°C, at 70°C and at 90°C (Fig.10). There was a similar evolution of MR for the time interval 0 to 20 min (t_1). Beyond 20 min, the kinetics of desorption at 70°C became faster than the one at 50 °C; the dry state was reached within 100 min (in t_2 of Fig.10) for 70°C and 150 min at 50°C (in t_3 of Fig.10). For the kinetic of 90°C, there was stabilizing trend around 50 min (t_4 of Fig.10).

The study has shown the thermal stability of C.S shellnut for the temperature up to 90°C; the sample do not show any form of crack. It's an advantage to use this bioresource as abrasive aggregate for sanding. Thus, it is also possible to use it as an abrasive for sanding ceramics in future research studies and even explore its use as aggregates in certain cement-based composite materials as such, it would be interesting to use it in sand [30] and powder form instead of the ships form of this present study.

3.5. Moisture adsorption and water absorption kinetics

The mathematical models shown in Table 2 were used to simulate the water and moisture absorption kinetics.

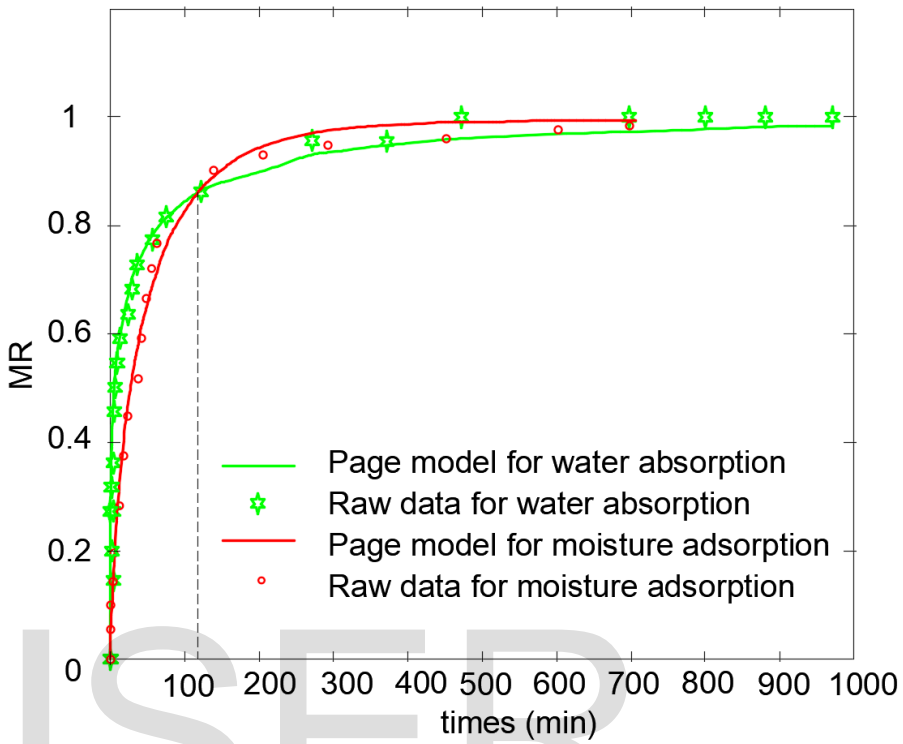

Figure 12. Predicted model of Page for moisture adsorption and water absorption.

The correlation coefficients for the different mathematical models are listed in Table 7. The most suitable model was Page's model for both moisture adsorption and water absorption (Fig 12). A similar result was found by Ndapeu et al. in their study of the water diffusion in CN, a material of the same type [30].

Table 7. Analysis of the drying performance of CS shellnut.

Kinetic		Adsorption	Absorption
Statistical indicator		R-Square	
Model	Number of Settings		
Page	3.0	0.966	0.989
Pilosof	3.0	0.932	0.983
Peleg	2.0	0.932	0.970
Sikame et al	5.0	0.906	0.989
Mohsenin	4.0	0.928	0.987

The parameters of the model for CS are presented in Table 7.

Table 8. Calculated parameters of Page model for the adsorption and absorption kinetics

Settings	a	k	n
Moisture adsorption	1.03	0.14	0.37
Water absorption	0.93	0.01	0.73

The absorption diffusion was lower than adsorption. This is justified by the fact that in the first 1000 minutes of kinetics, gaseous molecules are lighter and easier to be capture than liquid molecules. The overall saturation percentage of absorption was evaluated as 30.13%: this is relatively close to the saturation percentage for the adsorption kinetics. This CS water absorption value is higher than the saturation percentage of CN which was 17.32% of species 1 and 20.42% of species 2 [30]. This higher diffusion rate is due to the porosity of these materials and the microstructure.

3.6. Effective coefficients of diffusion for sorption (water absorption and moisture adsorption)

The values of effective diffusion coefficients were $2.98x10^{-11}$ ($\pm$ $2.81x10^{-12}$) $m^2.s^{-1}$ and 1.01×10^{-11} ($\pm1.09\times10^{-12}$) $m^2.s^{-1}$, respectively, for the moisture adsorption and water absorption kinetics. It was found that the diffusion rate for desorption at 50° C was higher than half that obtained for moisture adsorption at room temperature. The Brownian motion of the molecules is increasing with temperature, and therefore the diffusion [31]. The overall saturation percentage for sorption was evaluated as 29.5% (Eq. 5). This value is approximately three times the total absorption value of the recycled aggregates whose absorption in 24 hours is estimated at 10% [32]. To date, the literature proposes works on the substitution of natural aggregates with recycled aggregates. The CS could also integrate this campaign of substitution of natural resources.

3. Results

This paper focused in physical, water diffusion and micro-structural analysis of CS shellnut specimens. The shape of CS shellnut is ellipsoidal. SEM showed that the CS shellnut has very tight and closed clump-like cracks. With EDS analysis, it clear that the CS shellnut is light density (1.30) because it does not contain heavy element. Therefore, its particular form of porosity is an indicator of water diffusion kinetic. Understanding of the diffusion was obtained by carrying out experiments on the desorption, adsorption and absorption kinetics. The overall saturation percentage of absorption and adsorption from the anhydrous to the saturation state was around 30.13% to 29.50% respectively; the drying kinetic was done at three isotherms temperatures (50°C, 70°C and 90°C), while absorption and adsorption were performed at room temperature. For the drying kinetics, between the 7 models tested, Page's model was the most suitable mathematical model to predict the phenomenon. For the absorption and adsorption kinetics, between the 5 models tested, Page's model was the best mathematical model for the prediction of the phenomenon. The analytical solution of diffusion, Crank's equation, made it possible to determine the effective diffusion coefficient for the drying kinetics, for the absorption and adsorption according to experimental data. For drying, the effective diffusion coefficient for the three isotherms (50, 70 and 90°C) states were $2.70x10^{-11}$ ($\pm$ $2.18x10^{-12}$) $m^2.s^{-1}$ at 50°C and $29.71x10^{-11}$ ($\pm1.09x10^{-11}$) $m^2.s^{-1}$ at 70°C

and $39.00x10^{-11}$ ($\pm 2.51x10^{-11}$) $m^2.s^{-1}$ for 90°C. For the absorption and adsorption, the effective diffusion coefficients were $2.98x10^{-11}$ ($\pm 2.81x10^{-12}$) $m^2.s^{-1}$ and $1.01x10^{-11}$ ($\pm$ $1.09x10^{-12}$) $m^2.s^{-1}$ respectively. The Arrhenius's equation permitted determination of the activation energy for drying according to the three isothermal state that were evaluated, it was at 28.66kJ/mol.K. Hence, CS shellnut is positioned as a new organic material for composites. However, studies on the effect of grain size on the physical parameters have to be considered, as well as their mechanical and chemical characterizations.

Acknowledgements

The authors would like to thank the *Pan African Materials Institute* (PAMI) for facilitating the EDS testing during the *Pan African School for Materials* (PASMAT) program 2016. The authors would also thank the participation of Syrille Bryce Tchinwoussi and Jonathan Sesyi for their participation during the Lab's activities.

References

[1] V. Jacques and J.-J. Faure, *Fruitiers sauvages d'Afrique: (espèces du Cameroun)*. Clohars Carnoët: Editions Nguila-Kerou, 1996.

[2] O. E. Matig, O. Ndoye, J. Kengue, and A. Awono, *Les fruitiers forestiers comestibles du Cameroun*. Cotonou: IPGRI Regional Office for West and Central Africa, 2006.

[3] L. Temgoua, R. Njoukam, and R. Peltier, "Plantations ingénieuses de bois d ' œuvre par les paysans de l ' Ouest-Cameroun," *Bois forêts des Trop.*, vol. 309, no. 3, pp. 63–76, 2011.

[4] G. B. Nkouam, "Conservation des fruits du karité (Vitellaria paradoxa Gaertn.) et de l'aiéle (Canarium schweinfurthii Engl.) : isothermes de sorption d'eau et extraction des matières grasses des fruits stockés," Institut National Polytechnique de Lorraine, 2007.

[5] M. A. Nyam, M. D. Makut, J. U. Itelima, and A. M. Daniel, "Nutritional Potential of the Fruits of Black Olive (Canarium schweinfurthii Linn) from Plateau State , Nigeria," *Pakistan J. Nutr.*, vol. 13, no. 6, pp. 335–339, 2014.

[6] O. J. Abayeh, A. K. Abdulrazaq, and R. Olaogun, "Quality characteristics of Canarium schweinfurthii Engl. oil.," *Plant Foods Hum. Nutr.*, vol. 54, no. 1, pp. 43–8, 1999. https://doi.org/10.1023/a:1008080611964.

[7] R. Njoukam and R. Peltier, "L'aiélé (Canarium Schweinfurthii Engl .) : premier essai de plantation dans l'ouest du Cameroun," *Fruits*, vol. 57, no. 4, pp. 239–248, 2002. https://doi.org/10.1051/fruits:2002021.

[8] O. T. Tcheghebe, A. J. Seukep, and F. N. Tatong, "A review on traditional uses, phytochemical composition and pharmacological profile of Canarium schweinfurthii Eng," *Nat. Sci*, vol. 14, no. 11, pp. 17–22, 2016.

[9] U. Bassey *et al.*, "Adsorption Isotherm, Kinetics and Thermodynamics Study of Cr (VI) ions onto Modified Activated Carbon from endocarp of Canarium schweinfurthii," *Int. Res. J. Pure Appl. Chem.*, vol. 6, no. 1, pp. 46–55, 2015. https://doi.org/10.9734/IRJPAC/2015/14823.

[10] K. A. Maguie, N. J. Nsami, K. Daouda, C. N. Randy, and K. J. Mbadcam, "Adsorption Study of the Removal of Copper (II) Ions using Activated Carbon Based Canarium Schweinfurthii Shells Impregnated with ZnCl2," *IRA-International J. Appl. Sci. (ISSN 2455-4499)*, vol. 8, no. 1, p. 18, 2017. https://doi.org/10.21013/jas.v8.n1.p2.

[11] A. Olawale and O. Ajayi, "Thermal Activation of Canarium Schweinfhurthi Nutshell," *Aust. J. Basic Appl. Sci.*, vol. 3, no. 4, pp. 3801–3807, 2009.

[12] D. Ndapeu *et al.*, "Elaboration and Characterization of a Composite Material Based on Canarium schweinfurthii Engl Cores with a Polyester Matrix," *Mater. Sci. Appl.*, vol. 11, no. 03, pp. 204–215, 2020. https://doi.org/10.4236/msa.2020.113014.

[13] G. B. Noumi, S. Laurent, E. Ngameni, C. Kapseu, Y. Jannot, and M. Parmentier, "Modélisation de la déshydratation de la pulpe des fruits du Canarium schweinfurthii Engl," *Tropicultura*, vol. 22, no. 2, pp. 70–76, 2004.

[14] J. C. Ehiem, V. I. O. Ndirika, U. N. Onwuka, Y. Gariepy, and V. Raghavan, "Water absorption characteristics of Canarium Schweinfurthii fruits," *Inf. Process. Agric.*, vol. 6, no. 3, pp. 386–395, 2019.

[15] T. H. Nguyen, "Étude expérimentale et modélisation du procédé de séchage des végétaux," Thesis at Université de Bretagne-Sud, 2016.

[16] D. Ndapeu, E. Njeugna, S. B. Bistac, J. Y. Drean, M. Fogue, and J. N. Foba, "Experimental Study of the Drying Kinetics of the Coconut Shells (Nucifera) of Cameroon," *Mater. Sci. Appl.*, vol. 4, no. December, pp. 822–830, 2013.

[17] S. Lahsasni, M. Kouhila, and M. Mahrouz, "Adsorption-desorption isotherms and heat of sorption of prickly pear fruit (Opuntia ficus indica)," *Energy Convers. Manag.*, vol. 45, no. 2, pp. 249–261, 2004. https://doi.org/10.1016/S0196-8904(03)00133-X.

[18] H. Pehlivan, A. Ateş, and M. Özdemir, "Experimental evaluation of drying characteristics of sewage sludge and hazelnut shell mixtures," *Heat Mass Transf.*, vol. 52, no. 11, pp. 2367–2379, 2016. https://doi.org/10.1007/s00231-015-1751-8.

[19] A. Benghalem and J. M. Vergnaud, "Diffusion of a chemical through the liquid located in a polymer: Modelling and experiments," *Polym. Test.*, vol. 13, no. 1, pp. 35–45, 1994. https://doi.org/10.1016/0142-9418(94)90038-8.

[20] Y. Khatir, J. Bouzon, and J. M. Vergnaud, "Liquid sorption by rubber sheets and evaporation; models and experiments," *Polym. Test.*, vol. 6, no. 4, pp. 253–265, 1986. https://doi.org/10.1016/0142-9418(86)90003-6.

[21] P. Polyák, D. Szemerszki, H. C. Benke, and B. Pukánszky, "A novel method for the determination of diffusion coefficients in amorphous poly(3-hydroxybutyrate)," *Polym. Test.*, vol. 63, pp. 342–348, Oct. 2017. https://doi.org/10.1016/j.polymertesting.2017.08.037.

[22] A. L. Petrou, M. Roulia, and K. Tampouris, "The use of the Arrhenius equation in the study of deterioration and of cooking of foods - some scientific and pedagogic aspects," *Chem. Educ. Res. Pract. Eur.*, vol. 3, no. 1, pp. 87–97, 2002.

[23] J. Crank, *The mathematics of diffusion*, 2nd ed. London: Oxford University Press, 1975.

[24] E. Njeugna, D. Ndapeu, S. Bistac, J. N. Foba, and M. Fogue, "Contribution to the characterisation of the coconut shells (coco nucifera) of cameroon," vol. 4, no. 1, pp. 1–20, 2013.

[25] R. G. Elenga, G. F. Dirras, J. G. Maniongui, and B. Mabiala, "Thin-layer drying of Raffia textilis fiber," *BioResources*, vol. 6, no. 4, pp. 4135–4144, Aug. 2011. https://doi.org/10.15376/biores.6.4.4135-4144.

[26] T. Madhiyanon, A. Phila, and S. Soponronnarit, "Models of fluidized bed drying for thin-layer chopped coconut," *Appl. Therm. Eng.*, vol. 29, no. 14–15, pp. 2849–2854, 2009. https://doi.org/10.1016/j.applthermaleng.2009.02.003.

[27] E. M. F. Aquino, L. P. S. Sarmento, W. Oliveira, and R. V. Silva, "Moisture Effect on Degradation of Jute/Glass Hybrid Composites," *J. Reinf. Plast. Compos.*, vol. 26, no. 2, pp. 219–233, Jan. 2007. https://doi.org/10.1177/0731684407070030.

[28] A. Espert, F. Vilaplana, and S. Karlsson, "Comparison of water absorption in natural cellulosic fibres from wood and one-year crops in polypropylene composites and its influence on their mechanical properties," *Compos. Part A Appl. Sci. Manuf.*, vol. 35, no. 11, pp. 1267–1276, Nov. 2004. https://doi.org/10.1016/j.compositesa.2004.04.004.

[29] M. A. S. Spinacé, C. S. Lambert, K. K. G. Fermoselli, and M. A. De Paoli, "Characterization of lignocellulosic curaua fibres," *Carbohydr. Polym.*, vol. 77, no. 1, pp. 47–53, May 2009, doi: 10.1016/j.carbpol.2008.12.005.

[30] D. Ndapeu, E. Njeugna, N. R. Sikame, S. B. Bistac, J. Y. Drean, and M. Fogue, "Experimental Study of the Water Absorption Kinetics of the Coconut Shells (Nucifera) of Cameroun," *Mater. Sci. Appl.*, vol. 7, no. March, pp. 159–170, Mar. 2016. https://doi.org/10.4236/msa.2016.73016.

[31] A. Rudin and P. Choi, "Diffusion in Polymers," in *The Elements of Polymer Science & Engineering*, 3rd ed., San Diego: Academic Press, 2013, pp. 275–304.

[32] M. Houria and A. Nourredine, "Les granulats recyclés humidifiés : comportements des bétons frais et durcis," *XXIXe Rencontres Univ. Génie Civil. Tlemcen*, pp. 401–410, 2011.